

The detection of the $\lambda 2175 \text{ \AA}$ feature, and further analysis of the BAL line profile structure in the gravitational lens candidate UM425¹

Andrew G. Michalitsianos

NASA/GSFC Laboratory for Astronomy & Solar Physics
Code 680, Greenbelt, MD 20771

Emilio E. Falco

José A. Muñoz

Harvard-Smithsonian Center for Astrophysics
60 Garden Street
Cambridge MA 02138

Paul Hintzen

NASA/GSFC Laboratory for Astronomy & Solar Physics
Code 681, Greenbelt, MD 20771

Demosthenes Kazanas

Laboratory for High Energy Astrophysics
Code 661, Greenbelt, MD 20771

ABSTRACT

We obtained MMT spectra of the gravitational lens candidate UM425 to compare the redshifts and line profile structures of lens components A and B, which are separated by $\sim 6''.5$. The CIV $\lambda 1550 \text{ \AA}$ emission in both A and B exhibits Broad Absorption Line (BAL) structure, consistent with the earlier detection of BAL structure in OVI $\lambda 1033 \text{ \AA}$ and NV $\lambda 1240 \text{ \AA}$ that was found with the International Ultraviolet Explorer (IUE) in component A. Cross-correlation of the spectra of A and B using emission lines of CIV $\lambda 1550 \text{ \AA}$, HeII $\lambda 1640 \text{ \AA}$, NIII $\lambda 1750 \text{ \AA}$, CIII] $\lambda 1909 \text{ \AA}$ and MgII $\lambda 2800 \text{ \AA}$ reveals a difference in the redshifts of A & B. However, the detailed BAL line profile

¹Observations reported here were made with the Multiple Mirror Telescope Observatory, which is operated jointly by the University of Arizona and the Smithsonian Institution

structure found in spectra of A & B are strikingly similar to one another, which suggests the system is lensed. The spectra of A & B also indicate significant dust extinction, which we base on the presence of the λ 2175 Å absorption feature in the rest frame of the QSO ($z_{QSO} = 1.47$). This feature is commonly seen in galactic sources, but is not generally observed in QSO spectra. Our spectra show the presence of the λ 2175 Å absorption feature in spectra of both images associated with the gravitational lens UM425. Based upon the strong similarity of BAL line profile structure exhibited by UM425A&B, particularly the presence of the λ 2175 dust absorption feature in spectra of both images, we conclude that UM425 is a gravitational lens.

Subject headings: Gravitational Lenses — Dark Matter —
Quasars: individual (UM425)

1. Introduction

The wide angular separation found in a modest population of gravitationally lensed quasars suggests lensing by foreground clusters. The gravitational lens candidate UM425 = 1120 + 019 consists of two widely separated images ($\sim 6''.5$) which were first detected by Meylan & Djorgovski (1988, 1989). A suspected foreground cluster at $z \sim 0.6$ is a possible lens candidate, although evidence for its existence was not found in the Hubble Space Telescope (HST) Snap Shot Survey (Maoz et al. 1993). The large difference in luminosity between components of 5.6 mag ($m_{VA} = 16.2$, $m_{VB} = 21.8$) corresponds to a large relative magnification factor of ~ 100 .

Spectra of UM425A that Michalitsianos et al. (1995, 1996) obtained with the International Ultraviolet Explorer (IUE) indicate pronounced Broad Absorption Line (BAL) structure in OVI λ 1033 Å and NV λ 1240 Å, consistent with peak outflow velocities that range up to ~ -12000 km s $^{-1}$. As such, UM425 is a member of the rare population of BAL QSOs with $z \gtrsim 1.5$ that are gravitationally lensed. A campaign to monitor the BAL high ionization line profile structure over timescales ~ 10 months with IUE indicated significant changes in the OVI BAL absorption trough occur primarily at velocities ≥ -4000 km s $^{-1}$, while absorption features at velocities ≤ -4000 km s $^{-1}$ were characterized by more modest fluctuations.

Meylan & Djorgovski (1989) estimated $z_{QSO} = 1.465$, based upon the CIII] λ 1909 Å line. The IUE spectra yielded a slightly larger $z_{QSO} = 1.471 \pm 0.003$, as estimated from the Ly α λ 1216 Å line. The IUE value is indistinguishable from our optical estimate; see below.

2. Data Analysis

We obtained spectra of UM425 A&B with the MMT and the Blue Channel spectrograph. Table 1 shows a log of the observations. The useful range of observed wavelengths was 3350 – 8000Å, with a resolution of 1.96 Å pixel $^{-1}$ and an effective resolution (FWHM) of 7 Å. We calibrated the flux in the object spectra with spectra of the spectrophotometric standards GB191B2B and PG1545+035 that we acquired on the same night (see Table 1). The calibrated MMT spectra for components A and B are overplotted in Figure 1. These two spectra are a combination of 2 exposures, 2700 s each, for a total integration time of 1.5 hr.

We found a significant redshift difference between images A and B. Using IRAF task emsao, we find the following redshifts for the two components (based only on the high-SNR emission lines listed within parentheses): $z_A = 1.471 \pm 0.002$ (SiIV, CIV, HeII, CIII] and

MgII), and $z_B = 1.477 \pm 0.002$ (SiIV, CIV, HeII, NIII, CIII] and MgII). To confirm the disagreement in these redshifts, we cross-correlated the spectra with IRAF task xcsao, with component A in the role of template; we obtained a well-defined peak in the correlation for velocity $v = 627.6 \text{ km s}^{-1}$ for component B with respect to A. To summarize, from the emission line measurements, $z_B - z_A = 0.006 \pm 0.003$; from the cross-correlation, $z_B - z_A = 0.005 \pm 0.001$.

We found two lines in component B, HeII $\lambda 1640 \text{ \AA}$, and NIII $\lambda 1750 \text{ \AA}$ with an amplitude that was very different from that of component A, especially for NIII, which is almost imperceptible in component A. To analyze this effect quantitatively, we calculated the maximum fluxes in the CIV, CIII], HeII, NIII lines after subtracting the continuum for the components A and B (see Table 2). Using these values, we also determined the flux ratios in the two components and the relative B/A ratio (see Table 3).

The ratio of amplitudes in the HeII emission line in each component is $B/A \sim 2$. In the case of NIII, $B/A \sim 35$. These differences are clear in Figure 1, as is a very small shift in all the emission lines between the two spectra due to the redshift difference.

2.1. UV Resonance Lines

The CIV $\lambda 1550 \text{ \AA}$ line profile structure found in both lensed images indicates BAL outflow which provides further evidence that UM 425 is a lens. In Figure 2, OVI $\lambda 1033 \text{ \AA}$ obtained in an earlier epoch of UM425 A with IUE (Michalitsianos et al. 1996) is plotted on a common velocity scale with the CIV profiles from both lensed images in the $z_{QSO} = 1.471$ rest frame. The blue wings of both OVI and CIV show BAL structure in high ionization resonance that extends to velocities $V_{BAL} \sim -4000 \text{ km s}^{-1}$. However, we also note that the low ionization species MgII $\lambda 2800 \text{ \AA}$ is present only in emission. Absorption blueward of the emission profile is attributed to telluric water vapor. The lack of BAL structure in low ionization species UM 425 indicates UM425 is a high ionization BAL quasar. The distinct absorption line structure in both images strengthens the case that UM 425 is a lens because the probability of finding two BAL quasars within ~ 6 arcsec with very similar line profile structure is extremely small.

2.2. Absorption Structure

In Figure 1, a prominent broad absorption feature that is unrelated to the BAL lines can be seen in both UM425 A&B with a centroid wavelength of $\lambda 2175 \text{ \AA}$ (rest frame). This

corresponds to a redshift of $z_{abs} \approx 1.48$, essentially in the rest frame of the quasar. The measured equivalent width is $W_\lambda = 16.6 \text{ \AA}$ with a full base that depresses the continuum over $\sim 238 \text{ \AA}$. This feature corresponds to extinction that is commonly seen in galactic sources (Savage & Mathis 1979), but is not generally observed in QSO spectra. This absorption feature has not commonly seen quasar spectra and warrants further investigation. It may provide clues concerning the dust environs of the BALQSOs, particularly if it reflects foreground absorption by a dust torus or absorption in a host galaxy.

The presence of the $\lambda 2175 \text{ \AA}$ absorption feature provides a distinct feature that enables us to determine the reddening of the QSO and allows us to determine the continuous energy distribution of the QSO. This is important in order to determine the exact level of hydrogen ionization present in the BAL region because it relates to the excess metal abundances which are typically associated with BAL QSOs which indicate a high nitrogen abundance relative to hydrogen, carbon and oxygen and other metals.

2.3. Discussion

If UM425 is lensed, the difference in redshift between $z_A = 1.471 \pm 0.002$ and $z_B = 1.477 \pm 0.002$ from the emission lines of images A&B must be reconciled with similar complex line profile structure which is present in high-ionization ionic species. These observations established BAL line profile structure in image B, that follows from the line profile structure in high the resonance lines of CIV $\lambda 1550$. The BAL trough absorption is consistent with earlier IUE observations in the far-UV of UM425A that revealed high velocity outflow in OVI $\lambda 1033$ and NV $\lambda 1240 \text{ \AA}$. The blue edges of the BAL troughs in the far-UV lines in UM425 A indicate outflow with speeds that range up to $\sim -12000 \text{ km s}^{-1}$ in OVI $\lambda 1033$ and NV $\lambda 1240 \text{ \AA}$. The CIV BAL trough presents a narrower velocity range that indicates outflow at speeds that range up to ~ -4000 to -5000 km s^{-1} .

The measured differences in redshifts and amplitudes of several strong emission lines between images A & B may result from the intrinsic variations in the QSO. The wide angular separation between images of $\Delta\theta \sim 6''.5$ suggests a time delay of $\Delta t \sim 1.7$ years. This timescale is comparable to that for observed changes in BAL line profile structure of ~ 1 year observed in UM425 A with IUE (Michalitsianos et al. 1996). The emission components of the BAL lines are intrinsically broad, and changes in BAL absorption troughs that affect the blue wings of the line profiles may alter the observed wavelength centroid at different epochs of activity. This argument is purely speculative at present and further spectral monitoring is required to investigate this effect.

The lack of BAL structure in low ionization species such as MgII λ 2800 Å indicates UM425 is a reddened, high-ionization BAL quasar. The continuous energy distributions of low ionization MgII BALQSOs are usually affected by reddening from dust in the quasar (Turnshek et al. 1994); correcting for dust extinction in these sources is required in order to reconcile their continuum distributions with those of the high ionization BALQSO counterparts.

The presence of the λ 2175 Å absorption feature in both images in the rest frame of the quasar provides important information concerning the environs of the QSO. It also provides an additional feature that is common to both images and further evidence that UM425 is a lens. Reddening may result from foreground absorption by the host galaxy in which UM 425 is embedded, or from a pre-existing dust torus that surrounds the system. The presence of dust surrounding the BAL region is also important because it can affect the covering factor by scattering photons from the QSO, thus effectively increasing the global covering factor (cf. Turnshek et al. 1994).

Baldwin (1977) found an indication of λ 2175 Å absorption in QSO spectra of PHL938, Ton490, 3C286 and CTA102. Applying the Savage & Mathis (1979) galactic extinction law to these quasars, moderate extinction levels of $E(B-V) \sim 0.08$ for PHL938 and an $E(B-V) \sim 0.04$ for Ton490 were obtained. However, the majority of QSOs surveyed did not show the presence of the λ 2175 Å feature, while moderate to low levels of dust absorption were suggested from the observed continuum distribution in the survey.

The continuous energy distribution of the low ionization BALQSO PG 0043+039 was studied by Turnshek et al. (1994), who found reddening by dust at levels of $E(B-V) = 0.14$ that are similar to the extinction level found here. Correcting with the SMC extinction law, Turnshek et al. (1994) obtained HI column densities $\sim 4.4 \times 10^{21} \text{ cm}^{-2}$. However, the means by which the formation of dust grains proceeds and the manner by which grains survive the ionizing environment of the BAL region remains obscure. Shielding by the BAL clouds and the geometry of BAL outflow very likely are key components for explaining the presence of dust in these systems (Voit et al. 1993).

We applied the galactic Savage & Mathis (1979) law to the UM425 spectra based upon the presence of the λ 2175 Å dust feature. An $E(B-V) \sim 0.1$ was obtained, or $A_v \sim 0.3$, which is similar to the extinction level found for the low ionization BALQSO PG0043+339 by Turnshek et al. (1994). Without correcting for dust extinction in UM425, the continuous energy distribution between $\lambda\lambda 2045 - 3124$ Å in the $z_{QSO} = 1.47$ rest frame indicates a power law of $\lambda F_\lambda = -0.67$. Correction with an $E(B-V) = 0.1$ corresponds to a steeper spectral of $\lambda F_\lambda = -1.76$, which may reflect emission from a disc.

3. Summary and Conclusions

We obtained MMT spectra of both images of the gravitational lens candidate UM 425 to determine the relative redshifts of lines in the respective spectra, and to ascertain whether UM425 is lensed. We further explored the BAL line profile structure in both images previously observed only in the brighter image A ($m_V \sim 16.2$) with IUE ($m_V \sim 21.8$ for image B).

The MMT data confirmed BAL structure in the CIV λ 1550 Å line in both images, consistent with the source being lensed. Although a cross-correlation of the spectra of A and B restricted to the region containing the principal emission lines indicates differences in redshift of $z_B - z_A = 0.005 \pm 0.001$, based upon the centroid wavelengths of NIII, CIII], HeII, SiIV and MgII, the difference may be explained by the complex broad emission profile of BAL lines and changes in the BAL trough that can affect the emission profile at different epochs of observation, given the long delay time for the system of $\Delta t \sim 1.7$ years for images A & B. Temporal variability and the time delays for the 2 images may also explain the differences in line flux ratios for A & B shown in Table 3. However, more detailed monitoring is required to confirm this possibility.

The MMT spectra of both images in UM425 indicate the presence of dust extinction, as we deduce from the presence of the λ 2175 Å absorption feature observed in the rest frame of the quasar. Such a strong absorption feature in both images is strong evidence in favor of UM 425 being lensed, because the probability of finding 2 high-ionization BAL quasars within ~ 6 arcsec with very similar line profile structure is negligible.

We would like to thank Craig Foltz for establishing the connection among us. AGM would like to thank E. Dwek for useful discussions. JAM is supported by a postdoctoral fellowship from Ministerio de Educación y Cultura, Spain. We also thank the anonymous referee for correcting an error in the first version of our manuscript.

REFERENCES

- Baldwin, J. A. 1977, MNRAS 178, 67
- Maoz, D. et al. 1993, ApJ 409, 28
- Meylan, G. & Djorgovski, S. 1988, ESO Messenger 54, 39
- Meylan, G. & Djorgovski, S. 1989, ApJ 338, L1
- Michalitsianos, A. G. & Oliverson, R. J. 1995, ApJ 439, 599
- Michalitsianos, A. G., Oliverson & Maran, S. P. 1996, ApJ 458, 67
- Savage, B. D. & Mathis, J. S. 1979, ARA&A 17, 73
- Turnshek, D. A. et al. 1994, ApJ 428, 93
- Voit, G. M., Weymann, R. J. & Korista, K. T. 1993, ApJ 413, 95

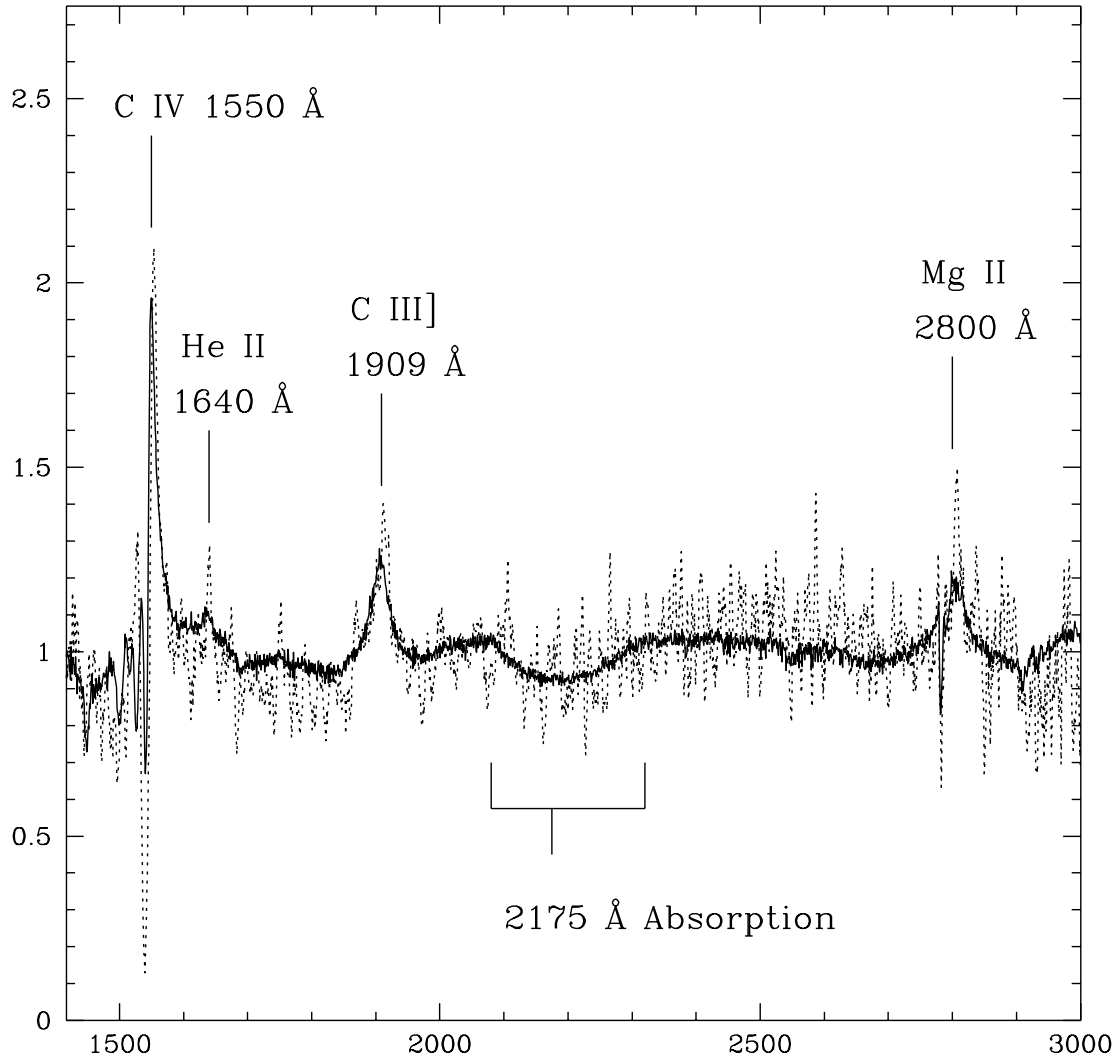


Fig. 1.— Calibrated spectra of the quasar UM425 (components A & B). Because of the large difference in luminosity between the two components, the spectra of A and B are normalized to a common scale for display purposes. The solid (dashed) line corresponds to the A (B) component. The abscissa shows observed wavelengths. Prominent emission lines, as well as the λ 2175 Å absorption are labeled.

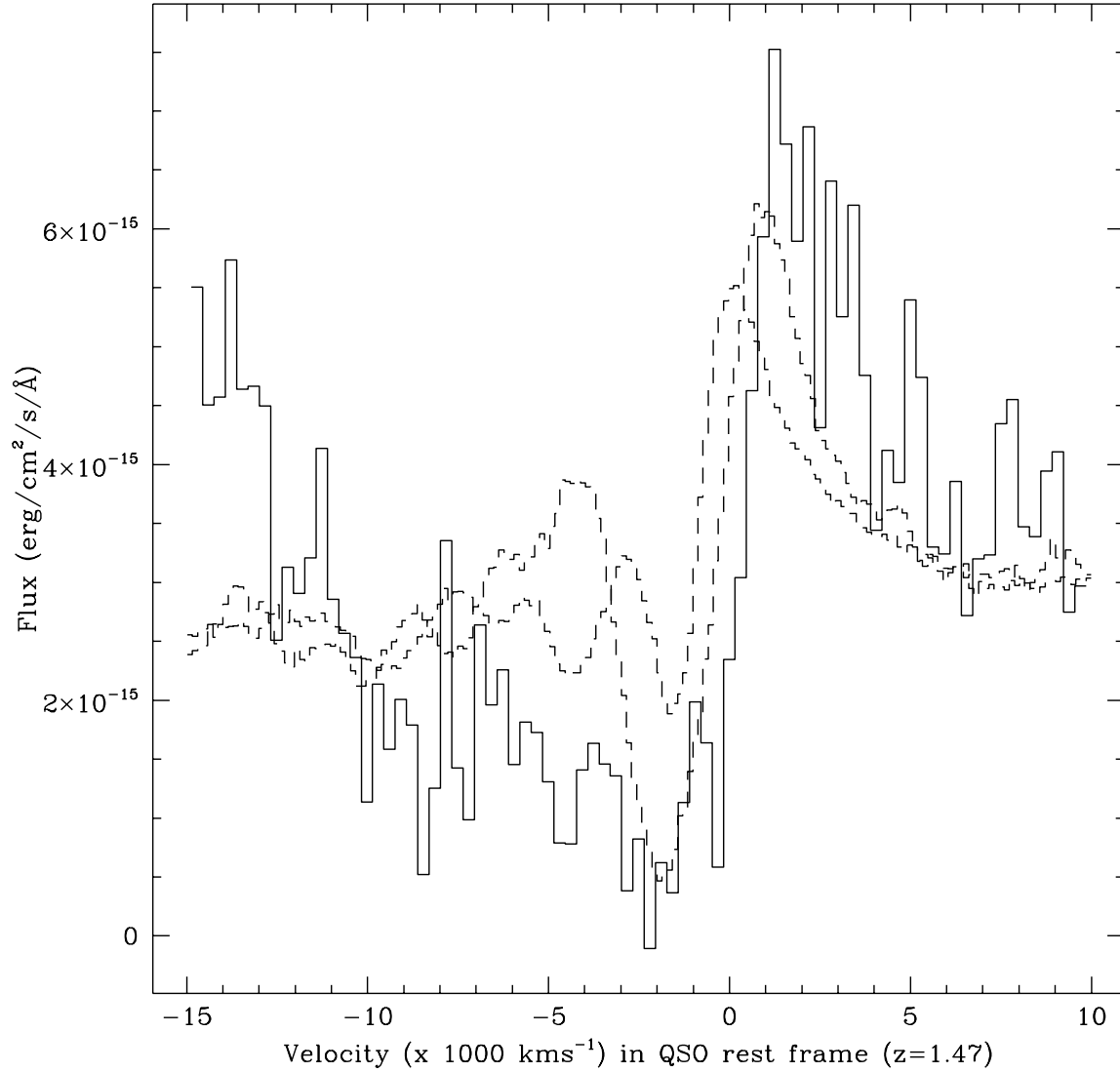


Fig. 2.— The OVI λ 1033 Å line profile (solid histogram) obtained from the IUE satellite (LWP29924) on 1995 Feb 7.6 (JD 2449,756.1) of UM425 A is plotted on a common velocity scale in the QSO rest frame, together with the CIV λ 1550 Å obtained of UM425 A (dashed upper curve) and UM425 B (lower dashed curve). The fluxes for CIV were scaled to a common level for display purposes. The abscissa shows velocities with respect to rest for component A.

Table 1. MMT observations log for UM425, UT 10 February 1997

No.	Object	Central λ Å	Exp. sec	UT	airmass	PA ° E of N	seeing FWHM "
1	UM425	6000	2700	7:54:04	1.25	-28.9	2.12
2	UM425	6000	2700	9:40:51	1.16	-28.9	2.15
3	GB191B2B	6000	30	1:53:57	1.10	0.0	1.58
4	PG1545+035	6000	30	13:14:25	1.15	0.0	2.12

Table 2. Line fluxes

	A	B
CIV	$1.494 \cdot 10^{-15}$	$2.705 \cdot 10^{-17}$
CIII]	$4.002 \cdot 10^{-16}$	$7.878 \cdot 10^{-18}$
HeII	$1.880 \cdot 10^{-16}$	$7.645 \cdot 10^{-18}$
NIII	$3.894 \cdot 10^{-18}$	$2.633 \cdot 10^{-18}$

Note. — Maximum fluxes after subtracting the continuum in components A and B, in $\text{erg}/\text{sec}/\text{cm}^2/\text{Å}$.

Table 3. Line flux ratios

	A	B	B/A
CIII]/CIV	0.27	0.29	1.07
HeII/CIV	0.13	0.28	2.15
NIII/CIV	0.0026	0.097	37.30
HeII/CIII]	0.47	0.97	2.06
NIII/CIII]	0.0097	0.33	34.02

Note. — Flux ratios for components A and B, and the ratio B/A.